MATHEMATICAL MODEL TO PREDICT PREHEATING TIME AND TEMPERATURE PROFILE IN BOXED-HEART SQUARE TIMBER DURING PREHEATING

Jing-Yao Zhao
Doctoral Candidate
E-mail: zjy_29445629@qq.com

Zong-Ying Fu
Doctoral Candidate
E-mail: fzy_1001@163.com

Xiao-Ran Jia
Doctoral Candidate
E-mail: jiaxiaoran1984@hotmail.com

*Ying-Chun Cai**
Professor of Wood Science and Technology
Key Laboratory of Bio-Based Material Science and Technology
College of Material Science and Engineering
Northeast Forestry University
Harbin, P.R. China
E-mail: ychcai@aliyun.com

(Received October 2014)

Abstract. The objective of this study was to develop a two-dimensional mathematical model that can be used to calculate the heat transfer in larch boxed-heart square timber during the preheating process. The preheating time obtained with the calculations agreed with the experimental results. Both experiments and calculations indicated that it took about 6.5 h for the center of the timbers (120 mm thick × 120 mm wide) to reach ambient temperature, suggesting that the model can be used to accurately estimate preheating times. During the preheating process, the simulated core temperature of the wood agreed with the experimental result. However, for the remaining locations, the relative error was rather large, with the value first increasing and then decreasing with time. Therefore, the model can only be used to accurately estimate temperature at the core region of the wood. Furthermore, the results suggested that MC had no significant effect on preheating time.

Keywords: Boxed-heart square timber, drying, preheating time, temperature profile, mathematical model.

INTRODUCTION

Preheating is a beneficial process in lumber drying (Gu and Garraham 1984). It can decrease drying defects and shorten drying time. For large cross-sectional structural lumber, preheating is especially important (Yamashita et al 2012, 2014). The main purpose of the preheating process is to increase the temperature of the wood core until it reaches the ambient temperature or target temperature. If the preheating process is insufficient, surface checks are easily created during the early drying stages. Conversely, if the process is excessive, it will result in a huge waste of energy. Therefore, setting up a scientifically validated and reasonable preheating process is important to ensure high quality and low energy consumption drying.

The preheating temperature, humidity, and preheating time are typically considered parameters

* Corresponding author

for the preheating process. Accurate determination of the time to reach the preheating temperature is especially crucial to ensure high quality of the drying process and decrease energy consumption. There are two main approaches to determine preheating time: the experimental method and the theoretical method (Hou et al 2000, 2002; Simpson et al 2003). Several studies have been published on the heating time of round and rectangular cross sections of wood and frozen wood (Simpson 2001; Li et al 2004; Cai 2005; Peralta and Bangi 2006; Cai and Oliveira 2010; Lv et al 2013). However, the theoretical estimation of the preheating time and the temperature profile related to boxed-heart square timber during the preheating stage has received little attention. Simpson (2004) developed a two-dimensional (2D) finite difference heat flow model that can be used to estimate the time required to heat the core of ponderosa pine and Douglas-fir square timbers to ambient temperature. But the temperature profile in the timber and the effect of MC on the temperature profile and preheating time has not yet been investigated.

Therefore, the objective of this study was to develop a 2D mathematical model that can be used to estimate the preheating time and temperature profile in larch boxed-heart square timber during the preheating process. The theoretical results were compared with experimental results, and influence of MC on preheating time and temperature profile was investigated.

Mathematical Model

During the preheating stage, wood is mainly heated through steam-heat transfer or convection from the heating coils plus steam heat to increase its core temperature to the target temperature. Because lumber length is normally much greater than its width and thickness, 2D approach was chosen for this study, which was then based on the following rational assumptions:

1. MC and temperature are constant and uniformly distributed at initial condition.
2. MC is almost constant during the preheating stage.
3. Heat is assumed to be transferred along thickness and width directions of the samples.
4. All specimen surfaces are exposed to the same external conditions, ie, the surface heat transfer coefficient is the same for all specimen surfaces.
5. The wood structure and the physical and chemical properties of the cross section are symmetrical, ie, the center layer acts as heat insulation.
6. The external environment, ie, the surface heat transfer coefficient, ambient temperature, humidity, and velocity, does not change with timber temperature.

Based on these assumptions, the governing equation of energy conservation is as follows:

$$\rho_d c_p \frac{\partial T}{\partial \tau} = \frac{\partial}{\partial x}\left(\lambda_x \frac{\partial T}{\partial x}\right) + \frac{\partial}{\partial y}\left(\lambda_y \frac{\partial T}{\partial y}\right) \qquad (1)$$

where T is temperature in °C, ρ_d is basic density of wood in kg m^{-3}, c_p is specific heat of wood in J·kg^{-1}·K^{-1} with $c_p = 2000 + 8.71MC + 4.98T$ (Steinhagen and Lee 1988), τ is time in s, x and y are distances along the thickness and width directions, respectively, in mm (Fig 1), and $\lambda = \lambda_x = \lambda_y$ is thermal conductivity along the x and y direction in W m^{-1} K^{-1} with $\lambda = (0.3248T + 1.11MC + 33.14)*10^{-3}$(Zhao et al in press).

Initial Condition

Based on Eq 1, the initial condition ($\tau = 0$) is as follows:

$$T(x, y) = T_0 \qquad (2)$$

where T_0 is initial temperature.

Boundary Conditions

For all values of τ, at $x = L = 60$ mm and $y = H = 60$ mm (surface), boundary conditions for the heat can be expressed by

$$\lambda \frac{\partial T}{\partial x} = h(T_e - T_s) \qquad (3)$$

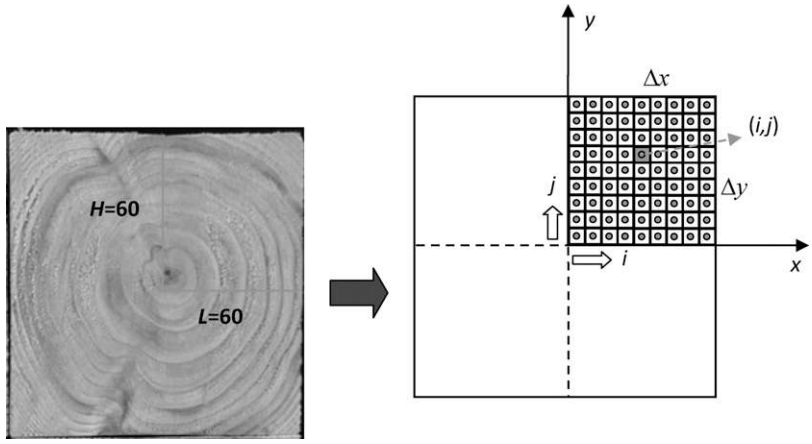

Figure 1. Illustration of the space discretization of the specimen's cross section (*x*-*y* plane).

$$\lambda \frac{\partial T}{\partial y} = h(T_e - T_s) \tag{4}$$

where h is heat transfer coefficient in $W \cdot m^{-2} \cdot K^{-1}$, T_e is ambient temperature in °C, and T_s is surface temperature in °C. Here, $h = 9.6$ (Zhao et al in press).

For all values of τ, at $x = 0$ mm and $y = 0$ mm (core) and based on Eq (5), it is assumed that no heat is transferred across the core center within the specimen. Thus, the boundary conditions for heat transfer can be expressed by

$$\frac{\partial T}{\partial x} = 0 \tag{5}$$

$$\frac{\partial T}{\partial y} = 0 \tag{6}$$

Other related parameters are given in the following section.

Numerical Solution

All the previously mentioned solutions of the partial differential equations were discretized using the control-volume approach. The *x*-*y* plane was constructed of discrete $I(i \times \Delta x) \times J(j \times \Delta y)$ units, with nodes located at the core of each unit (Fig 1). The time domain was divided into n equal parts, with a time step length $\Delta\tau$. To ensure that the equations could be solved, in general, the discretization was explicit, but the space and time step length had to be adjusted to ensure the stability of the algorithm.

With the control-volume method, as in Fig 1, the temperatures for the internal control volumes were calculated by

$$T(i,j,k+1) = T(i,j,k) + \left\{ \begin{array}{l} \Delta y\left[\lambda_{i+1,i,j}[T(i+1,j,k) - T(i,j,k)]/\Delta x + \lambda_{i-1i,j}[T(i-1,j,k) - T(i,j,k)]/\Delta x\right] \\ +\Delta x\left[\lambda_{i,j+1,j}[T(i,j+1,k) - T(i,j,k)]/\Delta y + \lambda_{i,j-1,j}[T(i,j-1,k) - T(i,j,k)]/\Delta y\right] \end{array} \right\} \Big/ A$$

where $A = \rho_d c_p(i,j,k)\Delta x \Delta y/\Delta\tau$, the harmonic averages of thermal conductivity, $\lambda_{1+1,i,j} = 2/(1/\lambda_{i+1,j} + 1/\lambda_{i,j})$, $2 < i < I - 1$, $2 < j < J - 1$.

The temperatures for the four boundary control volumes were calculated by

$$T(i,j,k+1) = T(i,j,k) + \left\{ \begin{array}{l} \Delta y\left[\lambda_{i,j+1,j}[T(i,j+1,k) - T(i,j,k)]/\Delta x + \lambda_{i,j-1,j}[T(i,j-1,k) - T(i,j,k)]/\Delta x\right] \\ +\Delta x\left[\lambda_{i+1,i,j}[T(i+1,j,k) - T(i,j,k)]/\Delta y\right] + h(T_d - T(i,j,k))\Delta x \end{array} \right\} \Big/ A$$

where $i = 1$, $2 < j < J - 1$.

$$T(i,j,k+1) = T(i,j,k) + \left\{ \begin{array}{l} \Delta y\left[\lambda_{i,j+1,j}[T(i,j+1,k) - T(i,j,k)]/\Delta x + \lambda_{i,j-1,j}[T(i,j-1,k) - T(i,j,k)]/\Delta x\right] \\ +\Delta x\left[\lambda_{i+1,i,j}[T(i+1,j,k) - T(i,j,k)]/\Delta y\right] \end{array} \right\} \Big/ A$$

where $i = \mathrm{I}$, $2 < j < J - 1$.

$$T(i,j,k+1) = T(i,j,k) + \left\{ \begin{array}{l} \Delta x\left[\lambda_{i+1,i,j}[T(i+1,j,k) - T(i,j,k)]/\Delta y + \lambda_{i-1,i,j}[T(i-1,j,k) - T(i,j,k)]/\Delta y\right] \\ +\Delta y\left[\lambda_{i,j+1,j}[T(i,j+1,k) - T(i,j,k)]/\Delta x\right] \end{array} \right\} \Big/ A$$

where $j = 1$, $2 < i < I - 1$.

$$T(i,j,k+1) = T(i,j,k) + \left\{ \begin{array}{l} \Delta x\left[\lambda_{i+1,i,j}[T(i+1,j,k) - T(i,j,k)]/\Delta y + \lambda_{i-1,i,j}[T(i-1,j,k) - T(i,j,k)]/\Delta y\right] \\ +\Delta y\left[\lambda_{i,j+1,j}[T(i,j+1,k) - T(i,j,k)/\Delta x] + h(T_d - T(i,j,k))\Delta y \right. \end{array} \right\} \Big/ A$$

where $j = \mathrm{J}$, $2 < i < I - 1$.

The temperatures for the four corner control volumes were calculated by

$$T(i,j,k+1) = T(i,j,k) + \left\{ \begin{array}{l} \Delta y[\lambda_{i,j+1,j}[T(i,j+1,k) - T(i,j,k)]/\Delta x] + h(T_d - T(i,j,k))\Delta x \\ +\Delta x[\lambda_{i+1,i,j}[T(i+1,j,k) - T(i,j,k)]/\Delta y] \end{array} \right\} \Big/ A$$

where $i = 1$, $j = 1$.

$$T(i,j,k+1) = T(i,j,k) + \left\{ \begin{array}{l} \Delta y[\lambda_{i,j+1,j}[T(i,j+1,k) - T(i,j,k)]/\Delta x] \\ +\Delta x[\lambda_{i-1,i,j}[T(i-1,j,k) - T(i,j,k)]/\Delta y] \end{array} \right\} \Big/ A$$

where $i = 1$, $j = J$.

$$T(i,j,k+1) = T(i,j,k) + \left\{ \begin{array}{l} \Delta y[\lambda_{i,j-1,j}[T(i,j-1,k) - T(i,j,k)]/\Delta x] + h(T_d - T(i,j,k))\Delta x \\ +\Delta x[\lambda_{i+1,i,j}[T(i+1,j,k) - T(i,j,k)]/\Delta y] + h(T_d - T(i,j,k))\Delta y \end{array} \right\} \Big/ A$$

where $i = 1, j = J$.

$$T(i,j,k+1) = T(i,j,k) + \left\{ \begin{array}{l} \Delta y[\lambda_{i,j-1,j}[T(i,j-1,k) - T(i,j,k)]/\Delta x] + h(T_d - T(i,j,k))\Delta x \\ +\Delta x[\lambda_{i-1,i,j}[T(i-1,j,k) - T(i,j,k)]/\Delta y] + h(T_d - T(i,j,k))\Delta y \end{array} \right\} \Big/ A$$

where $i = I, j = J$.

The program was executed in the Matlab-R2010b environment.

MATERIALS AND METHODS

Boxed-heart square timbers (3 m^3) with dimensions of 122 mm × 122 mm × 2 m cut from larch trees (*Larix gmelinii* Rupr.) with initial green MC for heartwood of 48% and for sapwood of 92% in the Heilongjiang Province in China were stored at the cold store before experiments. Temperature and RH in the cold store were 5.2 ± 0.4°C and 93.5 ± 5.1% RH, respectively. The main objective of cold storage before kiln-drying was to minimize initial MC variation of timbers. The low temperature and high RH inside the cold store could decrease MC variation in a timber as well as average MC of timbers.

To select different moisture contents of timbers, the running experiments were separated into two stages. Due to the variation of MC among timbers, different MC can be determined under the same cold store time. Thus, for the first experimental stage, the average moisture contents of timber in cold storage for 2 mo were 62.9 and 50.6%, respectively. For the second experimental stage, the average MC of timber stored in the cold store for 6 mo was 35.8%. Because of the cold store, the difference in MC from interior to exterior of the timber was decreased effectively. And the proportion of sapwood in cross section was relatively small (Fig 1). Thus, Eq (1) was rational. The two experimental stage conditions were exactly the same. Two timbers with similar moisture contents were placed in the same group (three groups in total) and were then cut and wrought into 18 specimens with dimensions of 120 × 120 × 600 mm (Fig 2a). Initial MC and basic density of the specimens in different groups are shown in Table 1. Average MC was determined using the oven-dry weighting method. All specimens were end-coated with silicone and metal foil to ensure that heat transfer occurred along the cross section. Based on data from previous publications (Yamashita et al 2012), the preheating temperature was set to 80-90°C. Initial temperature of the timbers ranged from 17 to 19°C.

The experiments were performed in a DS-408 conditioning chamber, in which the specimens were preheated at set conditions (dry-bulb temperature

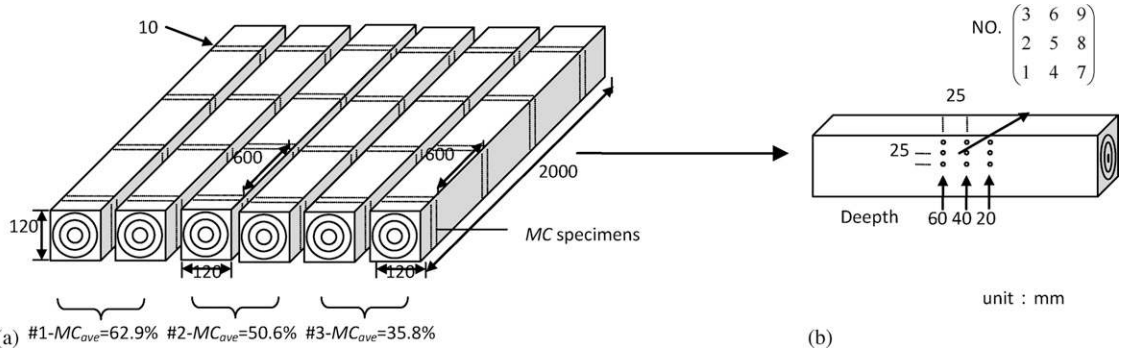

Figure 2. Diagram of sawing.

Table 1. Initial MC (MC) and basic density of the timber in different groups.

Group	MC_{avg} (%)	MC (%)		Basic density (kg m^{-3})	
		Min	Max	Average	SD[a]
1	62.9	58.8	69.4	445.3	43.0
2	50.6	46.5	54.6	430.4	33.5
3	35.8	30.5	40.2	421.4	49.3

[a] SD, standard deviation.

$T_d = 85 \pm 1.5$°C, wet-bulb temperature $T_w = 84.5 \pm 1.5$°C). Air velocity through the stack was approximately 2.0 m s^{-1}. Before preheating, nine 2-mm-diameter holes were drilled from the edge at different distances to the specimen surface, and then all specimens were weighed. A 1.4-mm-diameter thermocouple was placed in each hole, and then a round toothpick and silicone were used to seal the hole. Locations of the thermocouples in the specimen are shown in Fig 2b.

Because of the limited number of channels in the temperature recording instrument, the temperature of two specimens was recorded during each run and the other locations were filled with waste specimens (Fig 3). For each run, the experiment was repeated three times.

When the core temperature of the specimen had reached ambient temperature, the runs were stopped and preheating time and specimen weights were recorded. MC of the specimens decreased by approximately 3% during the preheating process. Temperature was recorded at time intervals of 1 min using an NEC (Itasca, IL) Remote Scanner Jr. DC3100 with precision of 0.1°C.

Figure 3. Specimen stacking.

After the preheating experiments were completed, a small block (120 × 120 × 10 mm) was cut from the location of the thermocouples and used to determine basic density.

RESULTS AND DISCUSSION

Calculation of Temperature Distribution

Figure 4 shows the three-dimensional plots and contour plots for the temperature profiles at different moments during the preheating process for the specimens in Group 1. Each temperature, T, is the average of the temperatures calculated at the same position and moment for each of the six specimens in Group 1. As seen on the temperature profiles, the temperature of the specimen interior was lower than the temperature at the surface. Especially for the edges, the temperature was highest during preheating. This phenomenon conforms to the law of heat transfer. That is, the heat of the drying chamber is transmitted to the wood surface by convection and then transferred to the wood interior by thermal conduction. At the corners, some additive effects from the two adjacent sides of the specimens occurred. Results from the calculations are consistent with the heat transfer law and are stable without showing volatility. The numerical and experimental results are compared in the next section.

Calculation Results Compared with Experimental Results: Preheating Temperature

Numerical and experimental results are compared in Fig 5. However, it is difficult to analyze the details of the change and compare the heat transfer in each position. Therefore, Fig 5 only shows the temperature profile for nine locations in the specimen, as previously illustrated in Fig 2b. Figure 5 reveals that the numerical results for the positions 3, 6, 7, 8, and 9 (close to the surface) are obviously lower than the experimental results, but for positions 1, 2, 4, and 5, the calculated values are close to the experimental results. For the temperature of the

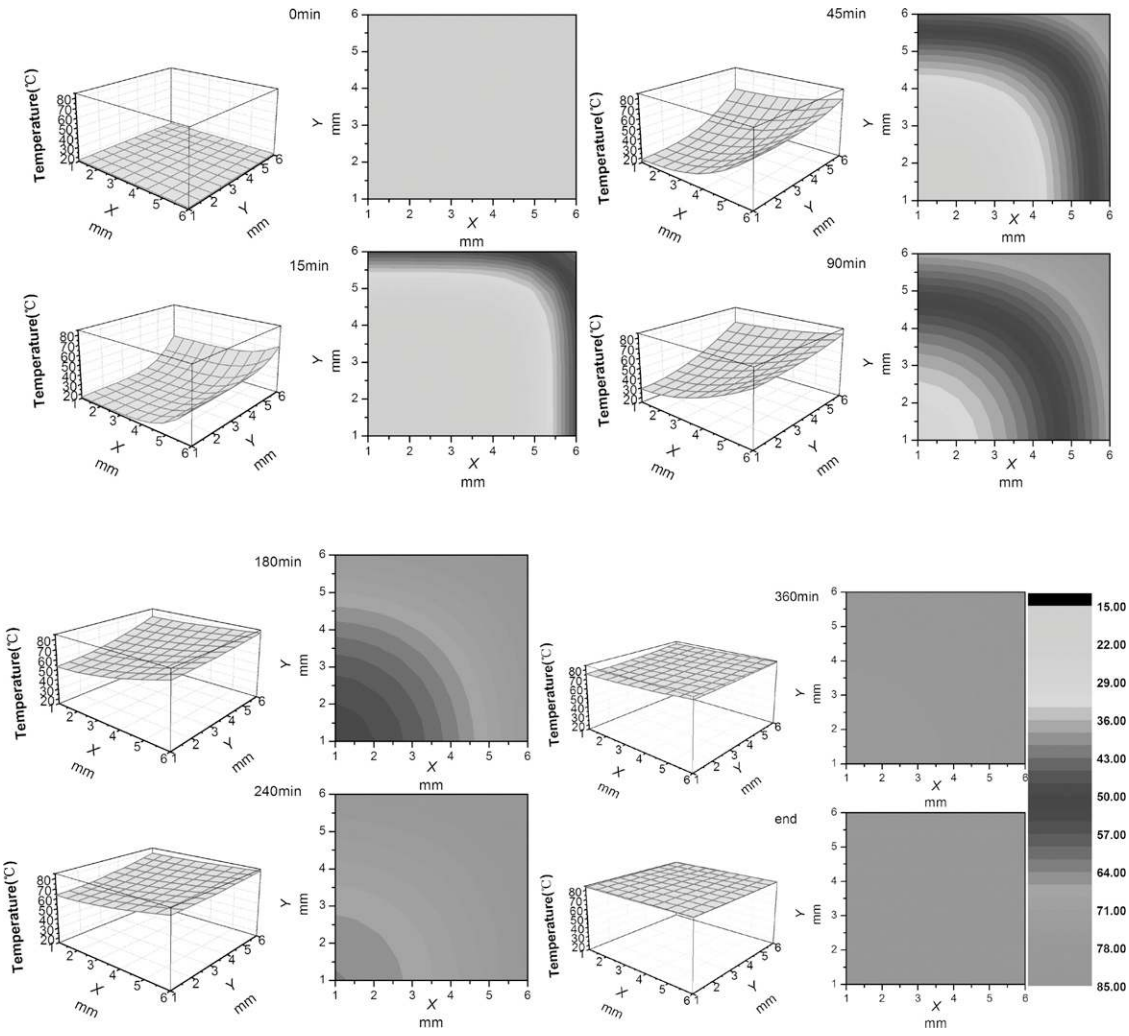

Figure 4. Temperature profile for different stages during the preheating process (Group 1 - $MC_{avg} = 62.9\%$).

core region, the calculation results agreed with the experimental results (average relative error $E_r = 3.4\%$, $E_r = (\text{Exp. } T - \text{Cal. } T)/\text{Exp. } T \times 100$). Therefore, the model can be used to predict the core temperature of the specimens.

During the preheating stage, the maximum value of E_r for each location obtained from the comparison between the numerical and the experimental results appears at $\tau = 25$–50 min and begins to gradually decrease afterward (Fig 6). This phenomenon is particularly obvious close to the specimen surface. The cause of E_r and its variation may be the existence of differences in wood properties and changes in MC. Changes in MC may be the main factor. During this stage, the ambient water vapor content was close to the saturation point. When the water vapor encountered lower temperature specimens at an early stage, some water vapor liquefying into liquid water molecules was adsorbed on the specimen and heat was released, increasing the surface temperature. As can be seen in Fig 7, experimental heating rate is particularly higher than numerical results. Probably because of this, MC of the specimens decreased by approximately

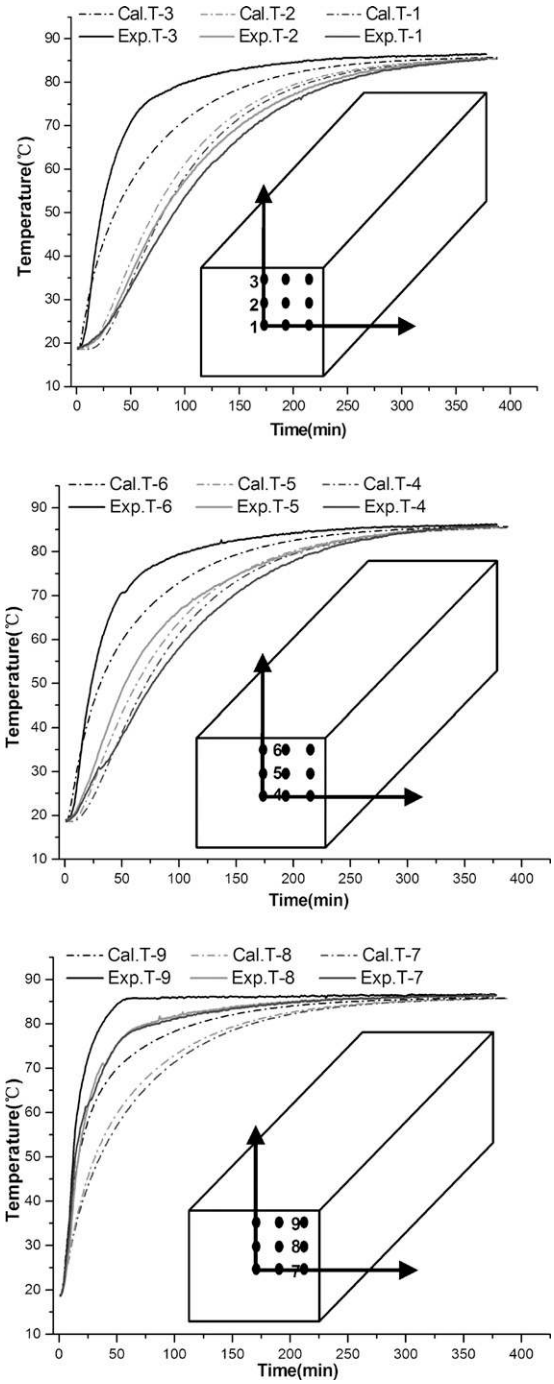

Figure 5. Comparison of the calculated temperatures (Cal. *T*) and the experimental temperatures (Exp. *T*) during the preheating process (Group 1).

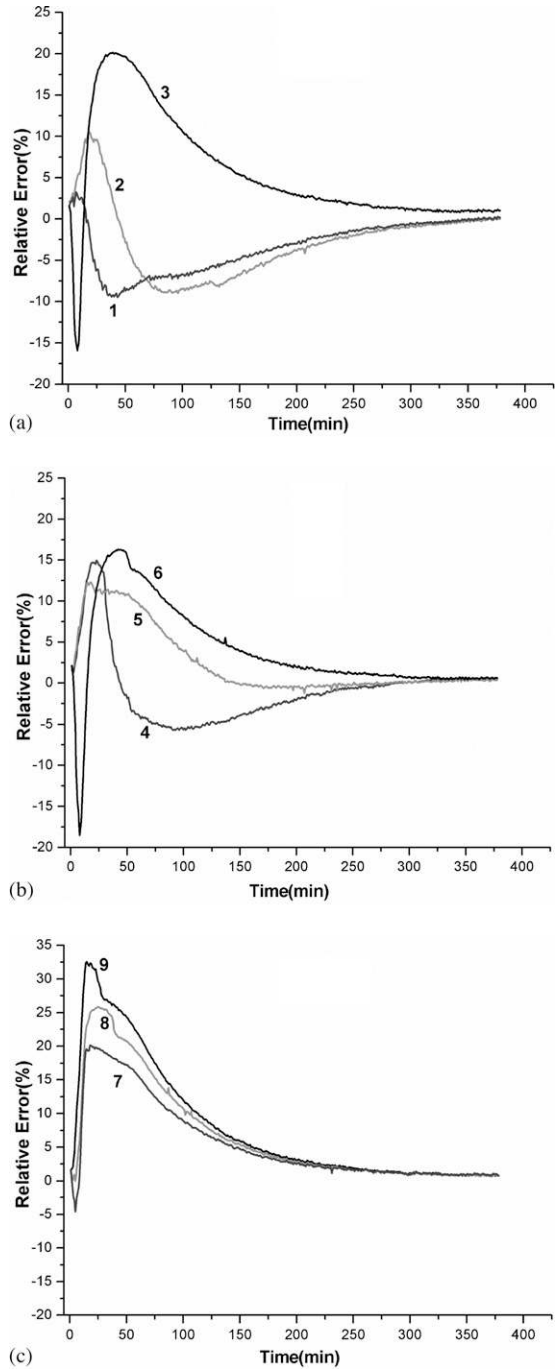

Figure 6. The relative error curves between the calculated values and the experimental values.

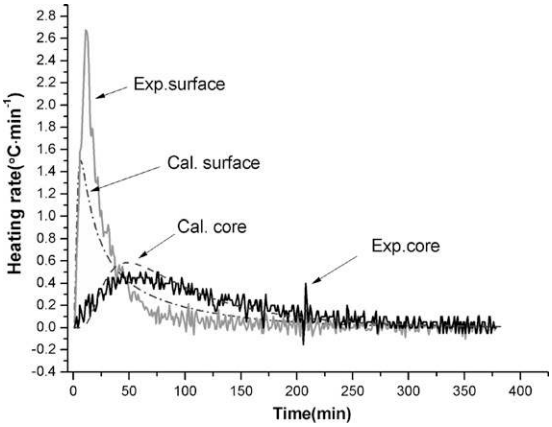

Figure 7. Comparison of the heating rates at the core region and surface position.

3% during the preheating process. Thus, Eq (2) was also rational. As the process continued, the surface temperature gradually reached ambient temperature, eventually leading to the end of the water vapor adsorption process. Because the MC of the specimen's surface was higher than the wood EMC (≈22%), water began to evaporate from the surface and the surface heating rate decreased sharply (Fig 7). Consequentially, the gap between the numerically and the experimentally determined heating rate gradually disappeared until the end of the preheating process.

As shown in Table 2, the E_r values for the numerical and experimental results for the different moisture contents were very similar and the volatility was small. The average E_r was 4.3%, and the standard deviation (SD) was 1.77%, suggesting that MC had little effect on the precision of the simulation.

Table 2. Statistical analysis of the relative error (E_r) between the calculation and the experimental values in different groups.

		E_r (%)			
Group	MC_{avg} (%)	Mean	Max	Min	SD[a]
1	62.9	5.01	32.6	0	1.9
2	50.6	4.52	28.6	0	2.0
3	35.8	3.37	23.5	0	1.4
Avg.	49.7	4.3	28.2	0	1.8

[a] SD, standard deviation.

According to these results and analysis, to optimize the simulation precision, an optimized model should consider differences in model relevant parameters, such as thermal conductivity and heat transfer coefficients, the wood properties, and changes in MC.

Calculation Results Compared with Experimental Results: Preheating Time

Values for the preheating times obtained through both calculations and experiments are shown in Table 3 and Fig 8. The calculations (376.8 min on average) agreed with the experiments (371.6 min on average), confirming the feasibility of predicting preheating time using the simulation model.

Table 4 shows that MC did not have a significant impact on preheating time. This result is consistent with data published by Li et al (2004) and Lv et al (2013). This phenomenon can be explained as follows: thermal conductivity of the wood increases with MC, facilitating a shorter preheating time. Conversely, the specific heat of the wood also increases with MC, ie, because of the rise in temperature, more calories are required per unit time, effectively

Table 3. Comparison of the preheating times obtained through calculations and experiments.

Group	MC_{avg} (%)	MC (%)	Exp. τ (min)	Cal. τ (min)	|Δτ| (min)	E_r[a] (%)
1	62.9	67.3	378	388	10	2.65
		62.1	351	367	16	4.56
		58.8	360	364	4	1.11
		69.4	403	365	38	9.43
		59.5	363	350	13	3.58
		60.1	382	367	15	3.93
2	50.6	51.1	391	370	21	5.37
		53.2	364	374	10	2.75
		46.5	374	376	2	0.53
		47.4	382	380	2	0.52
		50.9	390	373	17	4.36
		54.6	369	379	10	2.71
3	35.8	33.1	388	385	3	0.77
		30.5	382	382	0	0
		39.5	355	358	3	0.85
		34.4	378	351	27	7.14
		40.2	391	371	20	5.12
		36.9	381	388	7	1.84
Avg.	49.7	49.7	376.8	371.6	12.1	3.2

[a] E_r, relative error.

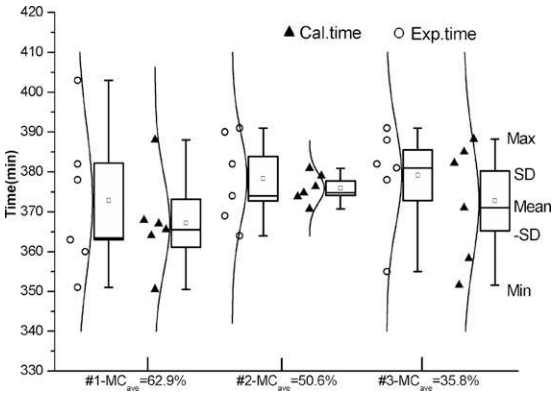

Figure 8. The box of calculation and experimental preheating time.

Table 4. Variance analysis for preheating time.

Source	Df	SS	MS	F	P
MC	2	142.11111^{Exp}	71.05556	0.33359	0.72153
		236.16444^{Cal}	118.08222	0.91781	0.42069
Error	15	3195^{Exp}	213	—	—
		1929.85167^{Cal}	128.65678		
Total	17	3337.11111^{Exp}	—	—	—
		2166.01611^{Cal}			

prolonging the preheating time. Values for the preheating time obtained through the numerical simulation and the experiments indicate that the two effects balance each other. For a complete preheating cycle only (without considering the effect of preheating on permeability and softening of the wood), the results of this study suggest that the preheating time can be set to approximately 6.5 h.

CONCLUSIONS

A 2D mathematical model based on the heat transfer law was developed to predict the preheating time and the temperature profile in larch boxed-heart square timber during the preheating process. The model was solved simultaneously using the control-volume approach, and the numerical and experimental results were compared. With an average and maximum relative error of 3.2 and 9.4%, respectively, the preheating time obtained through the calculations agreed with the experimental results. Both experiments and calculations indicated that it took about 6.5 h for the core of the lumber (120 mm thick × 120 mm wide) to reach ambient temperature, suggesting that the model can indeed be used to estimate preheating times. During the preheating process, the simulated core temperature of the wood agreed with the experimental results, with an average relative error of 3.4%. However, for the remaining locations, the relative error was rather large, with the value first increasing and then decreasing with time. Therefore, the model can only be used to accurately estimate the temperature at the core region of the specimen. Furthermore, the results suggested that MC had no significant effect on preheating time, but its changes had some effect on the temperature profile. In practice, to improve the simulation precision of the model, fluctuations of MC must also be considered.

ACKNOWLEDGMENT

This work was funded by the Chinese National Natural Science Foundation under Grant 31270595.

REFERENCES

Cai LP (2005) An estimation of heating rates in sub-alpine fir lumber. Wood Fiber Sci 37(2):275-282.

Cai LP, Oliveira LC (2010) Heating performance of frozen lodgepole pine lumber. Wood Fiber Sci 42(4): 467-473.

Gu LB, Garraham P (1984) The temperature and moisture content in lumber during preheating and drying. Wood Sci Technol 18(2):121-135.

Hou ZQ, Jiang XM, Guan N (2002) Theoretical determination of moisture and heat transfer to lumber during preheating. Wood Fiber Sci 34(2):287-292.

Hou ZQ, Jiang L, Hu JQ (2000) Theoretical analysis on the moisture flux and heat flux in process of wood preheating. Scientia Silvae Sinicae 36(3):103-109 (in Chinese).

Li XJ, Zhang BG, Yang T, Wang QX (2004) Determination of preheating time during wood drying. J Beijing For Univ 26(2):90-93 (in Chinese).

Lv L, Shi LC, Huang HB, Gao DH, You CJ, Yang LQ (2013) Factors affecting preheating time of oak lumber before drying. China Wood Ind17(3):51-53 (in Chinese).

Peralta PN, Bangi AP (2006) Finite element model for the heating of frozen wood. Wood Fiber Sci 38(2): 359-364.

Simpson WT (2001) Heating times for round and rectangular cross sections of wood in steam. Gen Tech Rep FPL-GTR-130 USDA For Serv Forest Prod Lab, Madison, WI. 103 pp.

Simpson WT (2004) Two-dimensional heat flow analysis applied to heat sterilization of ponderosa pine and Douglas-fir square timbers. Wood Fiber Sci 36(3):459-464.

Simpson WT, Wang X, Verrill SP (2003) Heat sterilization time of ponderosa pine and Douglas-fir boards and square timbers. Res Pap FPL-RP-607 USDA For Serv Forest Prod Lab, Madison, WI. 24 pp.

Steinhagen HP, Lee HW (1988) Enthalpy method to compute radial heating and thawing of logs. Wood Fiber Sci 20(4):415-421.

Yamashita K, Hirakawa Y, Saito S, Nakatani H, Ikeda M, Ohta M (2014) Effect of cross-sectional dimensions on bow and surface checking of sugi (*Cryptomeria japonica*) boxed-heart square timber dried by conventional kiln drying. J Wood Sci 60(1):1-11.

Yamashita K, Hirakawa Y, Saito S, Nakatani H, Ikeda M, Ohta M (2012) Masamitsu ohta surface-check variation in boxed-heart square timber of sugi (*Cryptomeria japonica*) cultivars dried by the conventional kiln drying. J Wood Sci 58(3):259-266.

Zhao JY, Fu ZY, Cai YC (2015) The study on inverse determination of thermal conductivity in wood with finite difference method. Scientia Silvae Sinicae (In press, doi:10.11707/j.1001-7488.20150000). (in Chinese).